

EFFECT OF INITIAL TURBULENCE ON VENTED EXPLOSION OVERPRESSURES FROM LEAN HYDROGEN-AIR DEFLAGRATIONS

Bauwens, C.R., and Dorofeev, S.B.

**FM Global, Research Division, 1151 Boston-Providence Turnpike, Norwood, 02062, USA,
carl.bauwens@fmglobal.com**

ABSTRACT

To examine the effect of initial turbulence on vented explosions, experiments were performed for lean hydrogen-air mixtures at elevated initial turbulence. As expected, it was found that an increase in initial turbulence increased the overall flame propagation speed and this increased flame propagation speed translated into higher peak overpressures during the external explosion. The peak pressures generated by flame-acoustic interactions, however, did not vary significantly with initial turbulence. When flame speeds measurements were examined, it was found that the burning velocity increased with flame radius as a power function of radius with a relatively constant exponent over the range of weak initial turbulence studied and did not vary systematically with initial turbulence. Instead, the elevated initial turbulence increased the initial flame propagation velocities of the various mixtures. The initial turbulence thus appears to act primarily by generating higher initial flame wrinkling while having a minimal effect on the growth rate of the wrinkles. For practical purposes of modeling flame propagation and pressure generation in vented explosions, the increase in burning velocity due to turbulence is suggested to be approximated by a single constant factor that increases the effective burning velocity of the mixture. When this approach is applied to a previously developed vent sizing correlation, the correlation performs well for almost all of the peaks. It was found, however, that in certain situations, this approach significantly under predicts the flame-acoustic peak. This suggests that further research may be necessary to better understand the influence of initial turbulence on the development of flame-acoustic peaks in vented explosions.

1.0 INTRODUCTION

Explosion venting is a method commonly used to minimize damage done to an enclosed structure following an accidental explosion. While engineering guidelines and standards exist to estimate the minimum vent size required for a given enclosure [1], these standards are not sufficiently reliable. Although other approaches exist [2, 3], several issues remain unresolved due to the complex nature of the phenomena and the limited set of existing experimental data on which they are based.

The difficulty in modeling vented explosions arises from the fact that the overall maximum pressure achieved during the explosion can be dominated by any one of a number of specific pressure transients [3, 4]. These transients correspond to different physical phenomena such as vent deployment, external explosions, increases in flame surface area due to obstacles, and the development of flame-acoustic oscillations. From previous studies, it was found that numerous parameters can affect each pressure transient. However, one parameter in particular, the burning velocity of the flame, controls the overall burning rate of the flame and should have a strong effect on all of the peaks.

The objective of the present work is to examine the effect of initial turbulence on the flame propagation velocity and peak overpressures that develop in vented explosions of hydrogen-air mixtures.

2.0 EXPERIMENTAL SETUP

Experiments were performed in FM Global's large-scale explosion test chamber. The test chamber has an overall volume of 63.7 m³, and a vent size of 5.4 m² is used for all of the tests. Prior to ignition, a thin plastic sheet was used to contain the unburned mixture and was perforated after mounting to

deploy evenly on three sides and produce a minimal (less than 0.5 kPa) deployment pressure. Ignition was supplied using a carbon rod igniter at a height midway between the chamber floor and ceiling. Two ignition locations were used in this study, one at the center of the chamber, center ignition (CI), and the other 0.25 m from the center of the wall opposite the vent, back-wall ignition (BW). Four chamber pressure transducers were mounted to the enclosure and a high-speed camera was used to measure the initial propagation velocity of the flame.

For this test series, hydrogen-air mixtures of varying concentration were used. The mixtures were sampled using a Cirrus mass spectrometer, which allowed the initial mixture concentration to be controlled to within an estimated accuracy of $\pm 0.5\%$ vol. The initial mixture was supplied by injecting fuel from the chamber floor while mixing fans were used to create a uniform mixture.

To generate the initial turbulent field, the mixing fans inside the chamber were used. Four, 0.5 m diameter mixing fans were used, with two mounted on each of the side walls of the chamber in a counterflow orientation. The decay of the turbulent field after the mixing fans were turned off was measured using a sonic anemometer at nine points throughout the enclosure. Once the decay of the turbulent field was characterized, the initial turbulent intensity for each test was set by varying the ignition delay after the fans were shut off. Figure 1 shows the decay of turbulent fluctuations inside the enclosure over time. These results are based on averaged fluctuations over multiple repeated measurements at the nine measurement points.

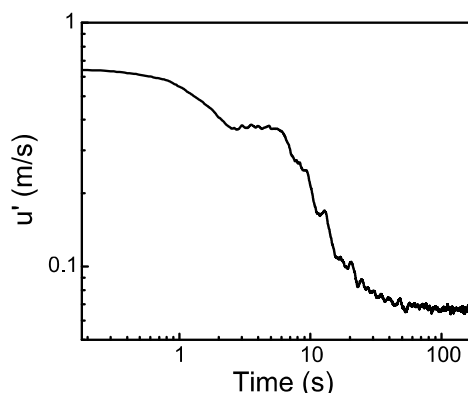


Figure 1. Decay of turbulent fluctuations inside the enclosure after shut off of mixing fans.

3.0 RESULTS

For this set of experiments, two main pressure peaks were observed. The first peak that develops is the external explosion peak, P_{ext} , where previously vented unburned gas is burned outside of the chamber. For the center ignition tests, a second peak develops later in time, P_{vib} , when flame-acoustic interactions develop within the enclosure.

Table 1 summarizes the peak pressures achieved during the vented explosion tests that were performed. In addition, a characteristic average flame propagation velocity, U_{ext} , defined as the distance from the ignition point to the vent divided by the time to the external explosion peak, is also given. This velocity represents the average flame propagation velocity between the time of ignition and the time the flame exits the chamber and can be used to estimate the relative burning velocity increase due to the elevated initial turbulence for tests where flame speed could not be measured directly. The table also includes the laminar burning velocity, S_L , and expansion ratio, σ , for each mixture that were used in the normalizations and calculations performed in the following sections.

Table 1. Summary of experimental results.

Test #	Conc (%)	Ign. Loc.	u' (m/s)	P_{ext} (bar)	P_{vib} (bar)	U_{ext} (m/s)	S_L (m/s)	σ
1	12.1	CI	0.09	0.003	0.009	3.8	0.17	3.98
2	12.4	CI	0.2	0.005	0.010	4.3	0.18	4.05
3	11.9	CI	0.4	0.009	0.011	4.4	0.15	3.92
4	12.3	CI	0.5	0.010	-	5.1	0.18	4.02
5	13.8	CI	0.2	0.011	0.019	4.8	0.28	4.38
6	15.0	CI	0.09	0.011	0.012	6.2	0.38	4.68
7	15.2	CI	0.12	0.014	0.016	6.3	0.39	4.72
8	15.1	CI	0.2	0.017	0.013	6.5	0.38	4.70
9	15.1	CI	0.4	0.019	0.017	7.0	0.38	4.70
10	14.9	CI	0.5	0.026	0.017	6.7	0.37	4.66
11	15.1	BW	0.09	0.046	-	9.6	0.38	4.70
12	15.0	BW	0.12	0.042	-	9.6	0.38	4.68
13	15.2	BW	0.4	0.052	-	10.6	0.39	4.72
14	14.8	BW	0.5	0.069	-	10.1	0.36	4.63
15	14.9	BW	0.5	0.060	-	10.9	0.37	4.65

Experimental pressure-time histories for the hydrogen-air mixtures are shown below in Figs. 2 and 3. These pressure signals were measured on the wall opposite the vent and were filtered using an 80-Hz low-pass filter to isolate potentially damaging pressure peaks. From these figures, it can be observed that the increased initial turbulent intensity also increases the propagation speed of the flame, seen by the earlier time to peak pressure, and the increase in magnitude of the external explosion peak. Over the range of values studied, however, the initial turbulence was found to have a minimal effect on the flame-acoustic peak. It is interesting to note that the flame propagation speed in the 15% hydrogen-air mixtures had a weaker response to elevated initial turbulence when compared with the 12% hydrogen-air mixtures. For example, an increase from $u' = 0.09$ m/s to $u' = 0.5$ m/s, in the 15% hydrogen-air tests, produced an increase in U_{ext} less than 15%. In the 12% hydrogen-air tests, the value of U_{ext} increased almost 35% over the same interval.

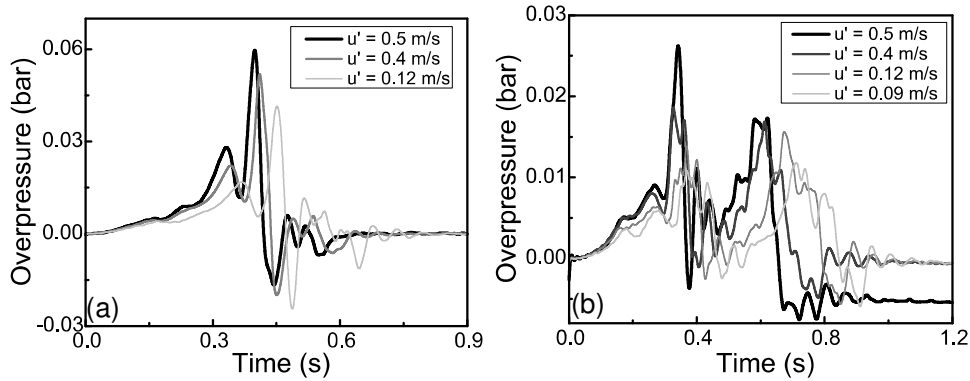


Figure 2. Experimental pressure time-histories of vented 15% hydrogen-air explosions for various initial turbulent intensities. Back-wall ignition (left) and center ignition (right).

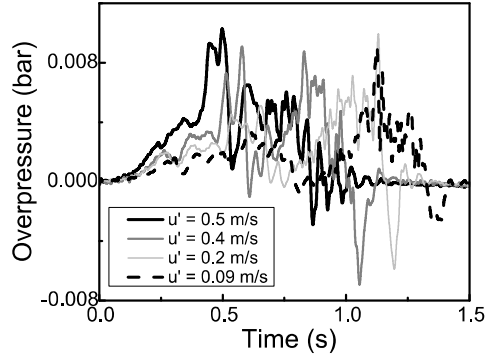


Figure 3. Experimental pressure time-histories of center ignition vented 12% hydrogen-air explosions for various initial turbulent intensities.

4.0 DISCUSSION

Figure 4 shows the values of both pressures peaks for the 12% and 15% hydrogen-air tests plotted as a function of u' . For both ignition locations and concentrations, both P_{ext} and P_{vib} tended to increase with increasing u' . It should be noted that there is one test, however, for a 12% center ignition test with 0.5 m/s initial turbulent fluctuations, where flame-acoustic interactions did not develop and a flame acoustic peak was not produced. With the exception of this test, the results for P_{vib} show little change (<0.005 bar) with u' for both mixtures over the range tested. This is interesting as previous studies with propane-air mixtures [5, 6] found unusual results where significantly higher P_{vib} was produced both at the low end and high end of the u' used in this study compared to intermediate values of u' . It is possible, however that these results are limited by the range of u' tested and that significantly higher or lower values of u' are needed for these hydrogen-air mixtures to produce the stronger P_{vib} peaks seen in the propane-air mixtures.

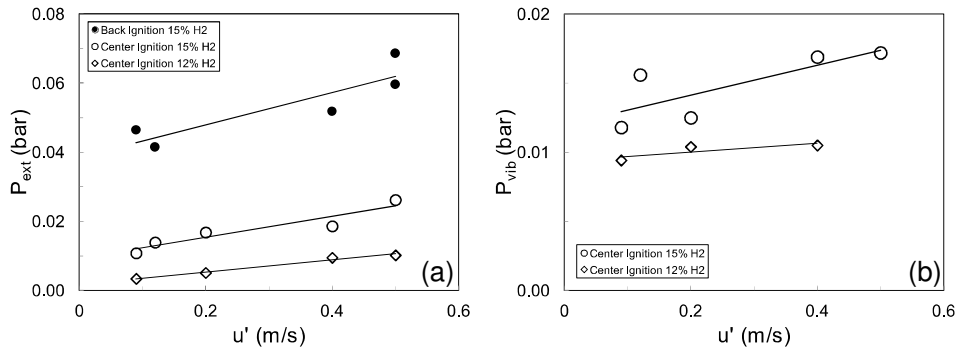


Figure 4. Variation in P_{ext} (left) and P_{vib} (right) with initial turbulence for hydrogen-air mixtures.

To help examine how the elevated initial turbulence affects flame propagation, Fig. 5a shows the average flame propagation velocity normalized by the expansion ratio which yields an estimate for the effective average burning velocity of the flame. In Fig. 5a, the two concentrations are seen to each vary linearly with $(u'/S_L)^{1/2}$ and are shifted vertically due to differences in both the laminar burning velocities as well as thermal diffusive effects. Back ignition tests were excluded from this figure due to the complex flame shapes that can develop for back ignition which are not directly comparable to the roughly spherical flames generated during center ignition. This linear trend is consistent with previous studies, which suggest that the turbulent burning velocity may be generally approximated to vary proportionally with $(u'/S_L)^{1/2}$ [7].

Figure 5b further normalizes U_{ext} by the laminar burning velocity the expansion ratio for each mixture. This figure isolates the contribution of turbulence and hydrodynamic flame instabilities, as a smooth, unwrinkled, spherical flame should produce $U_{ext}/S_L\sigma = 1$. From this plot, it is clearly seen that the effects of turbulence and thermal diffusive flame instabilities are significantly stronger in the leaner, 12% hydrogen-air mixture.

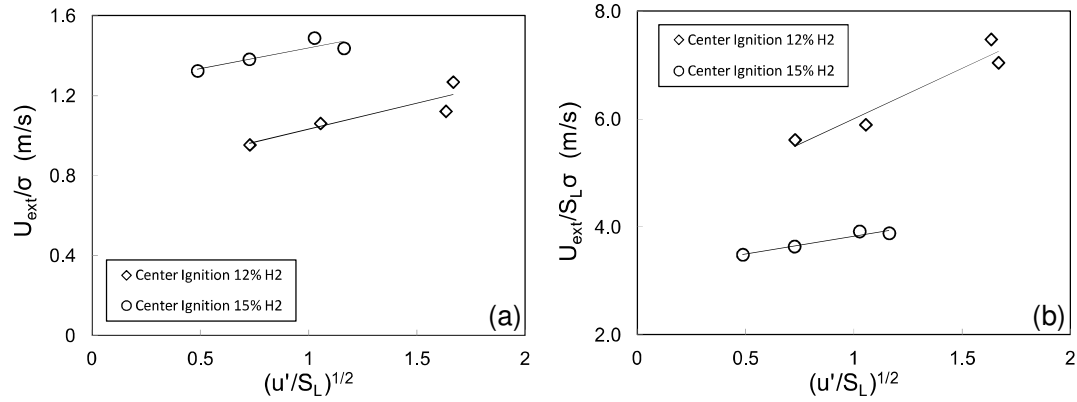


Figure 5. Average flame propagation velocity normalized by expansion ratio (left) and by the expansion ratio times the laminar burning velocity (right).

A plot where the average flame propagation velocity is normalized by the average flame propagation velocity for the same configuration at low initial turbulence, is shown in Fig 6. As the 12% hydrogen-air mixture had a lower laminar burning velocity, the value of $(u'/S_L)^{1/2}$ at $u'=0.09$ m/s was slightly higher than that of the 15% mixtures. To compare the results across the two mixtures, the 12% mixtures were normalized such that the points at $(u'/S_L)^{1/2} = 0.75$ coincided. In this plot, all three configurations examined fall on a single linear trend. This indicates that the relative increase in average flame propagation velocity due to turbulence may be the same across different concentrations and ignition locations. If this is the case, it would be possible to model the effect of turbulence based on the relationship at one concentration and extend the results across a range of initial concentrations and ignition locations as long as a baseline flame speed information for the concentrations and ignition locations are known.

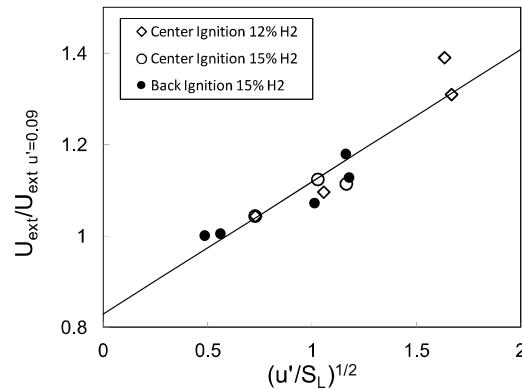


Figure 6. Average flame propagation velocity normalized by the average flame propagation velocity for same configuration at low initial turbulence, $u'=0.09$ m/s.

To further investigate how the initial turbulence affects the propagation speed of the flames, images from the high-speed camera were analyzed to measure the initial flame speeds for the center ignition hydrogen-air experiments up to a flame radius of 0.5 m. As the hydrogen-air mixtures did not produce sufficient visible light to directly capture the flame contour, a Background Oriented Schlieren (BOS)

technique [8] was used to reconstruct the flame shapes. These images were captured at a rate of 1,000 frames per second and flame contours were generated for each image, as illustrated in Fig. 7. For each flame contour, the cross-sectional area of the flame was calculated and corrected for the camera's view angle of the flame. The change over time of the average flame radius for the cross-section was then used to calculate the flame speed.

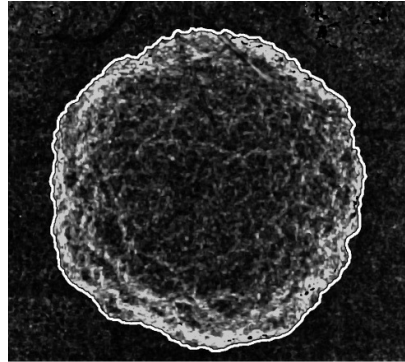


Figure 7. Example BOS image and calculated flame contour (white) used to estimate flame propagation velocity.

Figure 8 and 9 shows the measured propagation velocity of the center ignition 15% and 12% hydrogen-air flames as a function of flame radius. Power law fitted trend lines are also plotted with their associated coefficients. It is interesting to note that most of the fits indicate powers of roughly 0.3 and these values are consistent with those found in [9,10] that suggested powers between 0.20 and 0.33 for cellular spherical flames, where the increase of the burning velocity with distance was attributed to the hydrodynamic laminar flame instability. It is interesting to note that these powers are consistently higher than those observed for propane-air mixtures in a previous study [6] for nearly laminar flames which produced exponents closer to 0.25.

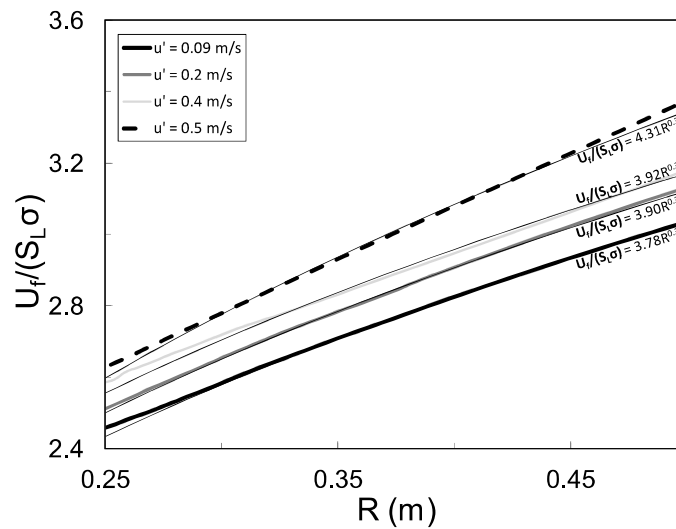


Figure 8. Observed flame speeds as a function of flame radius for a range of initial turbulence for center ignition 15% hydrogen-air mixtures.

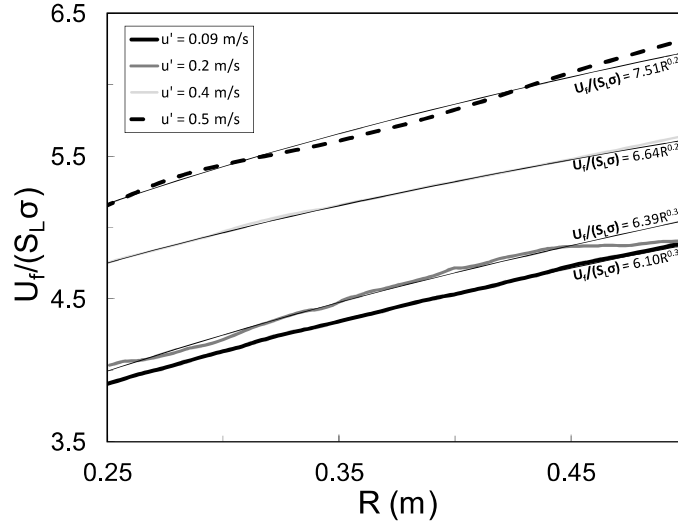


Figure 9. Observed flame speeds as a function of flame radius for a range of initial turbulence for center ignition 12% hydrogen-air mixtures.

In relation to the increase of the burning velocity with distance observed for weakly turbulent flames propagating through a gas mixture with pre-existing turbulence with $u'/S_L \leq 2$, (Figs. 8 and 9), the following observation can be made. The fact that the variations of the exponent do not follow a systematic trend for different turbulent intensities, suggests that, while the higher initial turbulence imparts higher initial flame wrinkling, the growth rate of the wrinkles is independent of the initial turbulence. It should be noted again that this observation may not be valid for a wider range of turbulent intensities and scales.

Similar findings follow from Figs. 10, which shows that changes in hydrogen-air mixture composition may be analogous to changes in initial turbulence. This is further illustrated using propane-air data from a previous study [6] in Fig. 11. For the varying hydrogen-air and propane-air mixture concentrations, changes in flame propagation velocity are primarily dominated by changes in the laminar burning velocity of the mixture and the thermal diffusive effects. The Lewis numbers of the 12.4%, 13.8%, and 15.2% were estimated as 0.27, 0.28 and 0.3, respectively, while the Lewis numbers of the propane-air mixtures are close to unity for mixtures of 3.7% ($Le > 1$) and for 4.2% ($Le < 1$). For mixtures of 4.2 - 6%, Le numbers decrease with concentration approaching values close to 0.87 for a 6.0% mixture. The laminar burning velocities for the propane-air mixtures were estimated to be 0.36, 0.39, 0.39, 0.33, 0.22, 0.17 and 0.13 m/s for the 3.7 - 6.0% mixtures accordingly. All the flames in Fig. 10 and 11 were visibly wrinkled soon after ignition due to the combined effect of turbulence and thermal-diffusive instabilities. For the varying hydrogen-air and propane-air mixture concentrations, changes in flame propagation velocity (and the effective turbulent burning velocity) are primarily dominated by changes in the laminar burning velocity of the mixture and the thermal diffusive effects that can develop in lean hydrogen-air and rich propane-air flames, as those mixtures have a Lewis number (Le) less than one. This is consistent with the observations reported in [11] where the effect of thermo-diffusive instabilities on turbulent burning velocities for a wide range of fuels are analysed. The exponent in the power function of burning velocity versus flame radius for the various hydrogen-air and propane-air concentrations also remains within a narrow range for each fuel respectively without a systematic trend for the different Le numbers. This implies that thermal-diffusive effects for the mixtures with $Le < 1$ appear to effectively create an initial baseline flame wrinkling, while their growth rate is independent of the Lewis number. This is consistent with the results of a previous study [12], where it was found that changes to the effective burning velocity, due to Lewis number effects, could be accounted for by scaling the mixture's laminar burning velocity by a single, measurable, value which is constant for each concentration. This is also consistent with analysis in [11] where it was noted that turbulent burning velocities tend to be higher for $Le < 1$. For

practical purposes, the data of Figs. 8, 9, 10 and 11 suggest that it is possible to model the effect of relatively weak initial turbulence as well as the Lewis number (or more rigorously, the Markstein number, Ma) simply by scaling the effective burning velocity with a single constant value for each turbulent intensity and Le or Ma .

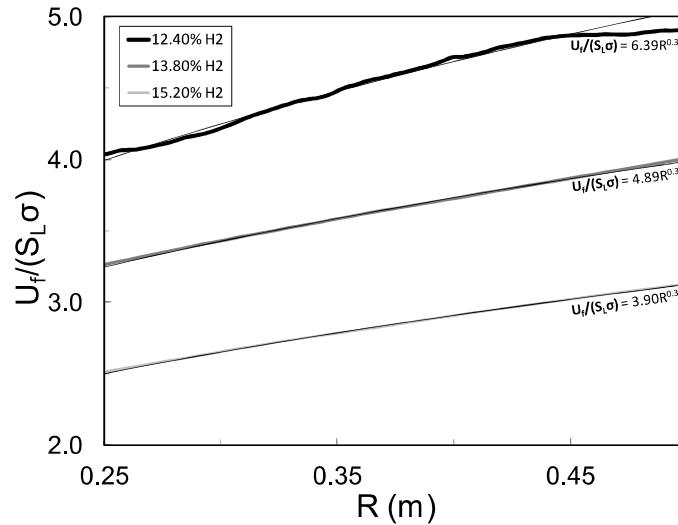


Figure 10. Observed flame speeds as a function of flame radius for a range of hydrogen-air concentrations.

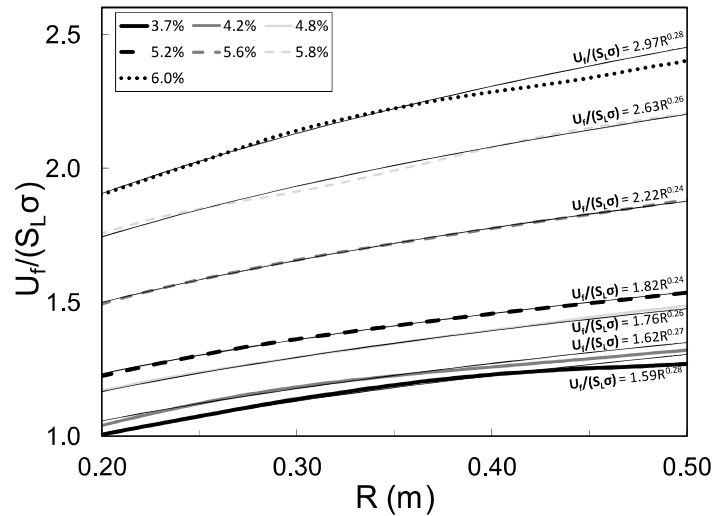


Figure 11. Observed flame speeds as a function of flame radius for a range of propane-air concentrations.

To test this hypothesis as applied to vented explosions, the pressure peak data can be compared with a previously developed vent sizing correlation [3,13,14] by simply modifying the effective burning velocity input parameter. As the initial burning velocity measurements were only readily available for the center ignition experiments, the effective burning velocity used in the correlation was estimated using U_{ext} . The estimated effective burning velocity was taken as the laminar burning velocity multiplied by the ratio of U_{ext} over $U_{ext}(u'=0.09)$, which was the baseline for low initial turbulence that was used in the previous studies performed in the 63.7 m³ enclosure.

The results of this modification, where the estimated effective burning velocity values are applied to the correlation, is shown in Fig. 12. For reference, this figure also includes results from the previous propane-air study [6]. It can be seen that reasonable agreement between the experimental and estimated results for the external explosion peak is found. In addition, the estimated results show good agreement with most of the flame-acoustic peak pressures and all of the hydrogen-air peaks. However, two of the flame-acoustic peaks, corresponding to the propane-air tests with the highest and lowest initial turbulence, are under estimated by a factor of three. It is possible that a similar trend may be observed for hydrogen-air mixtures if significantly higher or lower u' levels were tested. This shows that further examination of the effect of initial turbulence on flame-acoustic interactions may be necessary to properly describe the phenomena and may also explain some of the past difficulties in correlating the flame-acoustic peak from different experimental setups where different intensities of initial turbulence may have been present [14].

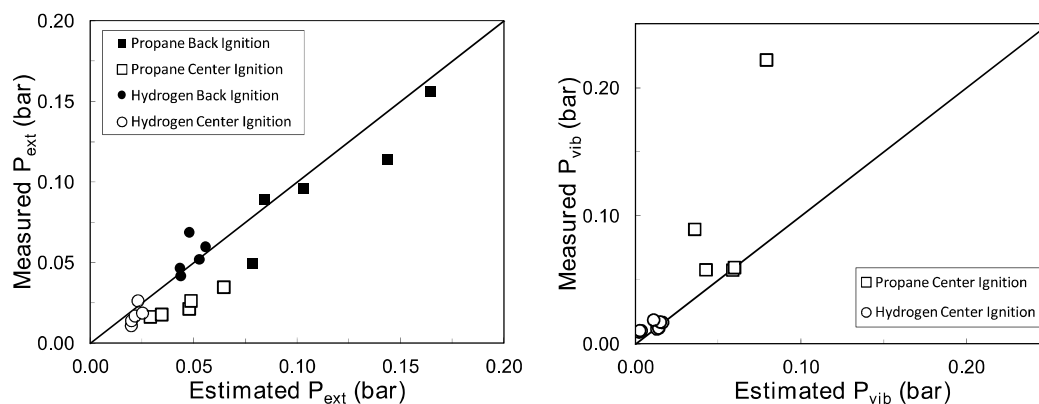


Figure 12. Comparison between measured peak pressures calculated based on an existing correlation using estimated effective burning velocities. P_{ext} (left) and P_{vib} (right).

5.0 CONCLUSIONS

Experiments were performed examining the effect of initial turbulence on vented propane-air and hydrogen-air explosions. As expected, it was found that an increase in initial turbulence increased the flame propagation speed for the hydrogen-air mixtures. This increased flame propagation speed translated into higher peak overpressures during the external explosion. Slightly higher flame-acoustic pressures were also observed at elevated turbulence levels, however, over the range of initial turbulence used in this study, these values did not vary significantly (<0.005 bar).

The flame speeds measurements of the hydrogen-air experiments show that the burning velocity increases with flame radius as a power function of radius with the exponent in the range of 0.3. This exponent appears to be roughly the same for different hydrogen concentrations and different turbulence levels (for relatively weak turbulence where $u'/S_L < 2$). The initial turbulence thus appears to act by creating initial flame wrinkling while the growth rate of the wrinkles is independent of the initial turbulence. The same is true for the thermal-diffusive effects when the mixture Lewis number is less than one, which appears to create baseline flame wrinkling, while the growth rate of the wrinkles is independent of the Lewis number.

For the practical purpose of modeling flame propagation and pressure generation in vented explosions, the increase in burning velocity due to both turbulence and Lewis number effects is suggested to be approximated by a single constant factor. When the different burning velocity factors observed in the experiments are applied to a previously developed vent sizing correlation, the correlation for the external explosion peak performs well across all of the data presented. The correlation also matches the flame-acoustic peaks well for hydrogen-air mixtures, however, previous studies with propane-air mixtures suggest the possibility of under prediction for turbulence levels outside the range studied.

The findings of this study can be applied to produce better predictions of vented explosion overpressures for scenarios where initial turbulence is expected.

REFERENCES

1. National Fire Protection Association, NFPA 68, Standard on Explosion Protection by Deflagration Venting, 2007, Quincy, MA 02269.
2. Molkov, V.V., Innovative Vent Sizing Technology for Gaseous Deflagrations, Proceedings of the Sixth International Symposium on Fire Safety Science, 5-9 July 1999, Poitiers.
3. Bauwens, C.R., Chaffee, J., and Dorofeev, S.B., Effect of Ignition Location, Vent Size and Obstacles on Vented Explosion Overpressures in Propane-Air Mixtures, *Combust. Sci. Tech.* **182** No. 11-12, 2010, pp. 1915-1932.
4. Cooper, M.G., Fairweather, M., and Tite, J.P., On the Mechanisms of Pressure Generation in Vented Explosions, *Combustion and Flame*, **65**, 1986, pp. 1-14.
5. Tamanini, F. and Chaffee, J.L., Turbulent Vented Gas Explosions With and Without Acoustically-Induced Instabilities, *Proc. Comb. Inst.* **24**, 1992, pp. 1845.
6. Bauwens, C.R. and Dorofeev, S.B., Effect of Initial Turbulence on Vented Explosion Overpressures, Proceedings of the Seventh International Seminar on Fire and Explosion Hazards, 5-10 May, 2013, Providence, Accepted.
7. Bradley, D., Lau, A.K.C., and Lawes, M., Flame Stretch Rate as a Determinant of Turbulent Burning Velocity, *Phil. Trans. R. Soc. Lond. A*, **338** No. 1650, 1992, pp. 359-387.
8. Meier, G.E.A., New Optical Tools for Fluid Mechanics, Proceedings of the Eighth Int. Symp. Flow Visualization, 1-4 September, 1998, Sorrento.
9. Gostintsev, Y.A., Istratov, A.G., and Shulenin, Y.V., Self-Similar Propagation of a Free Turbulent Flame in Mixed Gas Mixtures, *Combustion, Explosion and Shock Waves* **24**, 1989, pp. 563-569.
10. Wu, F., Jomaas, G., and Law, C.K., An Experimental Investigation on Self-Acceleration of Cellular Spherical Flames, *Proc. Comb. Inst.* **33**, No. 1, 2011, pp. 937.
11. Bradley, D., Lawes, M., Liu, K., and Mansour, M.S., Measurements and Correlations of Turbulent Burning Velocities Over Wide Ranges of Fuels and Elevated Pressures, *Proc. Comb. Inst.*, **34**, 2013, pp. 1519.
12. Bauwens, C.R., Chaffee, J., and Dorofeev, S.B., Vented Explosion Overpressures from Combustion of Hydrogen and Hydrocarbon Mixtures, *J. Hyd. Energy*, **36**, No. 3, 2011, pp. 2329.
13. Chao, J., Bauwens, C.R., and Dorofeev, S.B., An Analysis of Peak Overpressures in Vented Gaseous Explosions, *Proc. Comb. Inst.*, **33**, No. 2, 2011, pp. 2367.
14. Bauwens, C.R., Chao, J., and Dorofeev, S.B., Evaluation of a Multi-Peak Explosion Vent Sizing Methodology, Proceedings of the Eighth International Symposium on Hazards, Prevention and Mitigation of Industrial Explosions, 22-27 July, 2012, Krakow.